Numerical modeling of dielectrophoresis

by

Yuan Lin

May 2006
Technical Reports from
Royal Institute of Technology
KTH Mechanics
SE-100 44 Stockholm, Sweden

Akademisk avhandling som med tillstånd av Kungliga Tekniska Högskolan i Stockholm framlägges till offentlig granskning för avläggande av teknologie licentiatexamen onsdagen den 7:e Juni 2006 kl 13:00 i Sal D3, Kungliga Tekniska Högskolan, Vallhallavägen 5, Stockholm.

Universitetsservice US–AB, Stockholm 2006

Numerical modeling of dielectrophoresis

Yuan Lin 2006
KTH Mechanics
SE-100 44 Stockholm, Sweden

Abstract

We investigate the dielectrophoretic separation of microparticles. Two different models are formulated in two characteristic time scales. The first model mainly accounts for the orientation behavior and rotational motion of non-spheric microparticles. The concept of effective charge is suggested to calculate the finite size non-spheric particles. It is combined with the fluid particle dynamics method to calculate hydrodynamic as well as dielectrophoretic forces and torques. The translational motion and the particle-particle interaction are calculated also, but they take much longer time to be observed due to the different time scales of the rotational and translational motions

By viewing the particle as spheres, the second model focus on the translational motion of spheres. The hydrodynamic force between particles and particle-particle electrostatic interactions are also taken into account. We check the relative magnitude ratio between these forces in order to determine the importance of these forces. To predict and guide the design of experimental dielectrophoretic separation, two numerical applications are carried out. The first calculation suggests optimum patterns to improve the trapping efficiency of *E.coli.* cells by applying superimposed AC electric fields. The second calculation finds out the mobility and separation rate of particles which differs in size and electric properties by a multi-step trapping-releasing strategy.

Descriptors:
Dielectrophoresis, orientation of rotation, fluid particle dynamics, microparticle, molecular dynamics, hydrodynamics, particle-particle interaction, superimposed, mobility

Preface

This thesis contains the following papers:

Paper 1. Lin, Y. & Amberg, G. 2006 Simulation of dielectrophoresis of finite size particles. *Accepted by Proceedings of 2th International Conference on Transport Phenomena in Micro and Nanodevices (2006)*

Paper 2. Lin, Y., Amberg, G., Aldaeus, F. & Roeraade, J. 2006 Simulation of dielectrophoretic motion of microparticles using a molecular dynamics approach. *Accepted by Proceedings of ASME ICNMM 2006-4th International Conference on Nanochannels, Microchannels and Minichannels (2006)*

Paper 3. Aldaeus, F., Lin, Y., Roeraade, J. & Amberg, G. 2005 Superpositioned dielectrophoresis for enhanced trapping efficiency. *Published in Electrophoresis 26 (2005), 4252-4259*

Paper 4. Aldaeus, F., Lin, Y., Amberg, G & Roeraade, J. 2006 Multi-stepped dielectrophoresis for separation of particles. *Submitted to Journal of Chromatography A (2006)*

May 2006, Stockholm
Yuan Lin

Division of work between authors

Paper 1 is the work of Yuan Lin (YL), with the feedback from Gustav Amberg (GA).

In Paper 2, coding and calculations were done by YL, with the feedback from GA. GA suggested the idea of the model. YL did most of writing. Fredrik Aldaeus (FA) and Johan Roeraade (JR) provided experimental result and revised the paper.

In Paper 3, the idea of superposition electric field was suggested by FA and JR. YL did the coding and major part of calculation and the modeling part of writing with feedback from GA and FA. The minor part of calculation and major part of writing were done by FA with feedback from YL, JR and GA.

In Paper 4, the multi-step strategy was suggested by FA and JR. YL did the coding and major part of calculation with the feed back from GA and FA. FA did the writing and part of calculation with feedback from YL, JR and GA.

Contents

Part I

Overview and summary

CHAPTER 1

Introduction

Presently there is a strong trend towards miniaturizing equipment for chemical analysis and synthesis. This is made possible by development of technologies for fabricating small-scale structures that will serve as the components of a laboratory, such as pumps, valves, reactors, separators, *etc.* This is the lab-on-a-chip concept, where all of the components are built in a single device. Another trend is the design and manufacture of miniaturized mechanical components, such as miniaturized motors, valves, pumps, etc, often termed Electro Mechanical Systems (MEMS). The two have obvious connections in that pumps, valves etc and efficient fabrication methods are needed to implement a lab-on-a-chip. Often the manufacturing techniques have come from microelectronics, and have thus utilized silicon wafers etc, but also glass or plastics are used by Karniadakis and Beskok (2002). Also, as nano-technology progresses, there is a rapidly growing need to manipulate small objects, such as carbon nano-tubes, nanoparticles etc.

Microfluidics, which is essentially a field dedicated to miniaturized of plumbing and fluidic manipulation, offers the possibility of solving these issues for biology and chemistry. The fundamental fluid physics of fluid systems change rapid when the length scale decrease. A best-known phenomenon is that mass transport in microfluidic devices is dominated by the viscous dissipation and the inertial effects are generally negligible. This diminishes the instabilities caused by the nonlinearity of inertia. However, on the other hand, other physical phenomena of physics and chemistry become prominent such as electrostatics, thermodynamics, elasticity and so on, which rich microfluidics greatly.

Separation and deposition of cells and particles are of great interests in analytical chemistry, and which is an early application of microfluidic devices. The motivations are:

- Reduced sample consumption
- Size of cells or particle in the orders of magnitude are as chip (μm)
- Single particle manipulation
- Large electric field strengths with low voltages

In general, strategies used for the separation and deposition processes can be classified as follow:

- Mechanical (filters, micropipettes, etc)
- Magnetical
- Electric Electro-osmosis, Electrophoresis, Dielectrophoresis
- Flow cytometry (activated by fluorescence, magnetism, impedance, *etc*)

The different methods have their advantages and disadvantages therefore have different applied regions. This thesis focus in dielectrophoretic approach due to the specified application (cells and particles have close size and different frequency dependent electric properties, and are difficult to be separated by other methods).

For most applications involving micrometre and sub-micrometre particles, forces that tend to dominate in microdevices are viscous forces and electrical forces. Electrical forces can act both on particles and on the suspending fluid. The major electrical forces acting on small particles suspended in a fluid are electrophoresis and dielectrophoresis . Electrophoresis occurs due to the action of the electric field on the fixed, net charge of the particle, while dielectrophoresis only occurs when there are induced charges, and only results in motion in a nonuniform field (this can be a DC or an AC field) (Figure 1.1) During the

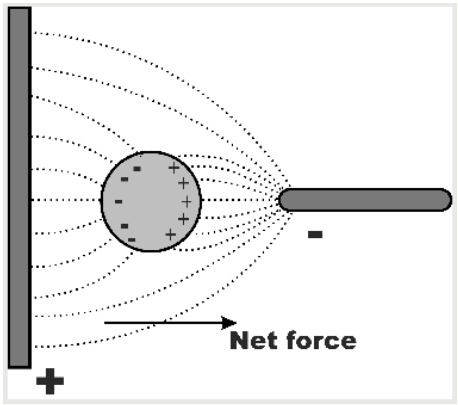

FIGURE 1.1. A schematic of a polarisable particle suspended within a point-plane electrode system. When the particle polarises, the interaction between the dipolar charges with the local electric field produces a force.

past four decades, dielectrophoresis has been studied in great detail. The term, "dielectrophoresis", is a combination of the word for force, "phoresis" from the Greek, and the word "dielectric". Pohl intended to use this term to describe the force exerted on uncharged dielectric particles by their polarizability, and his definitions are:

- Particles experience a DEP force only when the electric field is nonuniform.
- The DEP force does not depend on the polarity of the electric field and is observed with AC as well as DC excitation.
- Particles are attracted to regions of stronger electric field when their permittivity ϵ_p exceeds that of suspension medium ϵ_m, *i.e.*, when $\epsilon_p > \epsilon_m$.
- Particles are repelled from regions of stronger electric field when $\epsilon_p < \epsilon_m$
- DEP is most readily observed for particles with diameters ranging from approximately 1 to 1000 μm

An increasingly important application of DEP is in selective separation of bioparticles in lab-on-a-chip systems, and the feasibility of this has already been demonstrated for different cell types.

For example, Pohl (1978) demonstrated the separation of viable and nonviable yeast cells, and later he extended the experiments to separate other biological cells including canine thrombocytes, red blood cells, bacteria *etc.* Becker *et al.* (1995) performed separation of human breast cancerous cells from normal blood cells by a microelectrode array due to the large difference in dielectrophoretic properties of those cells, moreover, Gascoyne *et al.* (1997) did experiments to separate a various cancerous cells from blood cells and separated normal murine erythrocytes from erythroleukemia cells and measured their dielectric properties by changing frequency of the applied electric field [Gascoynea *et al.* 1997]. Markx *et al.* (1996) separated a mixtures of bacteria Bacillus subtilis, Escherichia coli and Micrococcus luteus.

There are several common strategies for dielectrophoretic separation in lab-on-chip systems. In flow separation, flow is used to carry two kind of different particles in a microchannel. One kind of particles are trapped on the electrode arrays located at the bottom of the channel, and the other would be brought out of channel by the flow. It has been demonstrated to be effective for separation of cancer cells [Becker *et al.* 1995]. The disadvantage of this strategy is, the cells are attracted to electrodes and need to be collected after separation. Therefore, strategies combined the separating and collecting processes are of interests recently.

Dielectrophoretic-field flow fraction is another strategy. The flow is introduced with different speed at different height from the bottom surface. Particles are repelled from the electrodes under a dielectrophoretic negative forces. The particles with different dielelctrophoretic properties would have different height therefore travel with different speeds with the flow. For example, Markx *et al.* (1997) employed this method in the separation of latex particles with different sizes, and Yang *et al.* (1999) performed the separation of human breast cells mixture with the blood cells. DEP-FFF takes use of velocity gradient in the

flow profile to achieve a high selective separation. However, the particles probably enter the channel with a Gaussian-shaped distribution which may causes overlap between the sub-populations of particles after separation.

Traveling wave dielectrophoresis is another recent and popular strategy in which electric fields rather than flow is used to give the particles a mean longitude velocity. That is, several applied electric fields are applied with continuous phase shift so that to give particles dielectrophoretic forces in both vertical and horizontal directions. In this case, the dielectrophoretic force expression is different from that given by Pohl (1951). The real part of Causius-Mossotti factor gives the DEP forces in vertical direction, while the imaginary part gives the DEP foces in horizontal direction (which is called the travelling force). This strategy has been demonstrated to separate erythrocytes and leukocytes cells [Morgan & Green 1997a].

The effect of Brownian motion was believed to be so large for submicron particles such that deterministic movement of submicron particles could not be achieved by using DEP. Pohl (1978) showed that excessively large electrical field gradients would be required to move a particle of 500 nm meter because the force on a particle due to Brownian motion increases as the particle's volume is reduced. However, in recent years, microelectrode photolithography technologies have been used to manufacture microelectrode arrays so it is able to produce strong electric fields from. These have been successfully used for the dielectrophoretic manipulation of a variety of nanoparticles [Green & Morgan 1999], nanorods, nanofibers [Asokan *et al.* 2003], deoxyribonucleic acid [Washizu *et al.* 1990], viruses [Morgan & Green 1997b], proteins [Washizu *et al.* 1994] and DNA [Asbury & Engh 1998]. More recently, DEP was used to separate metallic and semiconducting single-walled carbon nanotubes [Krupke *et al.* 2003a; Krupke *et al.* 2003b; Krupke *et al.* 2004].

For nanoparticles, several other effects become significant besides dielectrophoresis. For example the usage of high electric field strengths produces fluid flow and heating of the suspending electrolyte. The electric field can interact with the fluid to produce frequency dependent forces such as electro-osmosis and electrothermal force [Ramos *et al.* 1999; Hunter 1981]. The resulting flow exerts a drag force on the particles and produces an observable motion. Recently, a new type of force has been observed on microelectrodes due to the electric double layer (EDL) of a particle in an AC electric field [Ramos *et al.* 1999; Morgan & Green 2001]. EDL is also believed to enhance the dielectrophoretic effects on submicron particles and a simple model which combine EDL is suggested by Morgan & Green (2001). A thorough investigation about the models of EDL was done by Lyklema (1995).

Since the manufacture of microsystems is rather costly and measuring is also time-consuming, numerical modeling and simulation is very helpful for predicting the particle behavior in Dielectrophoresis and optimizing the design

of experiments. Most of the simulations done are based on the models of Jones (1995), who has developed simple and general models useful for predicting diverse examples of field-particle and particle-particle interactions based on the effective moment model.

In recent years, the distributed Lagrange multiplier method (DLM) suggested by Glowinski *et al.* (2001) was used to simulate the dielectrophoretic motion of microparticles and nanoparticles [Kadaksham *et al.* 2004; Kadaksham *et al.* 2005]. Theoretical studies about the dielectrophoresis of charged colloidal suspensions have been done by Huang *et al.* (2002). Numerical studies of using dielectrophoresis to separate and control carbon nanotubes have also been done by Dimaki & Bøggild (2004). All these simulations and numerical studies are based on the effective moment model.

CHAPTER 2

Theoretical preliminaries

2.1. Background of the model

Generally speaking, three main kind of analytical approaches have been used to calculate the DEP force and rotation torque on a biocell, which is usually modeled as a spherical homogeneous particle. The energy variation principle, used by Pohl (1951), described a lossless particle in a lossless medium. However, if the particle and medium are lossy, energy conservation law does not hold and this approach break down, as pointed out by Jones (1995).

The rigorous derivations of the DEP force and torque performed by Sauer (1983) are important from the standpoint of classical electrodynamics. Their analysis was based on a Maxwell stress tensor formulation integrated over the spherical surface of the particle in a lossy media under a slightly nonuniform electric field. The expansion of nonuniform electric field complicated the analysis greatly and caused severe mathematical difficulties. Therefore, the attention was only confined to a simple case of a homogenous sphere immersed in a dielectric liquid, and the applied electric field is just slightly nonuniform. It is hard to apply to many important practical cases of dielectrophoretic motions.

The main objective of this chapter is to introduce the effective dipole moment (EDM) method of calculating electromechanical forces and torques exerted by electric fields upon particles [Jones 1995] . The effective dipole moment method is valuable because it is easy to use and provides valid results in many important cases where rigorous derivations based on the Maxwell stress tensor seems difficult or impossible. Many topics such as the calculation of dielectrophoretic force, torque, orientation, employ this method.

Although the derivation of the effective dipole moment method is not rigorous, it is in complete agreement with the results obtained by Maxwell stress tensor integration for a homogeneous sphere with ohmic loss. In order to estimate the range of validity of force calculations based on the effective dipole moment approximation, Liu & Bau (2004) analytically solved cylindric and spherical particles in shells and in semi-infinite media by evaluating the Maxwell stress tensor, and compared with the results by effective dipole-moment method. They concluded that when $L/r > 20$ (where $L = |\mathbf{E}_0|/|\nabla \mathbf{E}_0|$), the dipole-moment approximation is accurate within better than 3%. Wang *et al.* (1997)

derived expressions for dielectrophoretic force and electrorotational torques for a homogeneous sphere in a nonuniform electric field based on the Maxwell stress tensor. They compared their results with those of the effective moment method and concluded that the discrepancy was only caused by the order of approximation.

2.2. Effective dipole moment

2.2.1. *Force on an infinitesimal dipole*

A dielectric material is a material that contains charges which polarize under the influence of an applied electric field. There are three basic molecular polarization mechanisms that can occur when a electric field is applied to a dielectric: electronic (the electron cloud moves), atomic (the ions move) and orientational (the permanent dipole moment changes direction) polarizations. However, none is regarded to be important in AC electrokinetics. The long-range interfacial polarization is viewed as playing an important role and is often referred as Maxwell-Wagner relaxation mechanism.

Interfacial polarization occurs because of a migration of charged carriers through the interfaces of dielectrics in such a way to produce different charge accumulations at the interfaces. It was first demonstrated by Maxwell and Wagner [Pohl 1978].

The starting point for formulating the force exerted on a dielectric particle is to estimate the net force upon a small physical dipole [Jones 1995]. The dipole consists of equal and opposite charges, $-q$ and $+q$.

If a nonuniform electric field is applied to a dipole with distance vector $\mathbf{d}$ between the charges, then the electric field at the two charges are not equal, and the sum of electric forces of the particle is:

$$\mathbf{F} = q\mathbf{E}(\mathbf{r}+\mathbf{d}) - q\mathbf{E}(\mathbf{r}), \tag{2.1}$$

where $\mathbf{r}$ is the position vector of $-q$. The electric field at the position of q can be expressed by Taylor expansion:

$$\mathbf{E}(\mathbf{r}+\mathbf{d}) = \mathbf{E}(\mathbf{r}) + \mathbf{d}\cdot\nabla\mathbf{E}(\mathbf{r}) + ... \tag{2.2}$$

Substituting 2.2 into 2.1, we obtain:

$$\mathbf{F} = q\mathbf{d}\cdot\nabla\mathbf{E} + ... \tag{2.3}$$

If high order gradients of the electric field are ignored, and since the dipole moment $\mathbf{p} = q\mathbf{d}$, the approximate expression of the force on the dipole is:

$$\mathbf{F} = \mathbf{p}\cdot\nabla\mathbf{E}. \tag{2.4}$$

2.2.2. *Derivation of EDM with ohmic loss*

A simple example is a homogeneous dielectric sphere of radius R, permittivity ϵ_p, and conductivity σ_p, immersed in a dielectric medium of permittivity ϵ_m

and conductivity σ_m. This system features one interface and one relaxation frequency.

The effective dipole moment $\mathbf{p}_{eff}$ of this particle, is defined as the moment of an equivalent, free-charge, point dipole that, when immersed in the same dielectric liquid and positioned at the same location as the center of the original particle, produces the same dipolar electrostatic potential. According to Jones (1995), the electrostatic potential ϕ due to a point dipole of moment in a dielectric medium with permittivity ϵ_m is of the form:

$$\phi(r,\theta) = \frac{qdP_1(cos\theta)}{4\pi\epsilon_m r^2} + \frac{qd^3P_3(cos\theta)}{16\pi\epsilon_m r^4} + ... \tag{2.5}$$

where P_1, P_3 are Legendre polynomial terms. If only the first term of the r.h.s. of (2.5) is considered, the approximation of electric field based on the effective dipole moment could be written as:

$$\phi(r,\theta) = \frac{\mathbf{p}_{eff}\cos\theta}{4\pi\epsilon_m r^2}, \tag{2.6}$$

where θ and $\mathbf{r}$ are respectively the polar angle and radial position in spherical coordinates. The derivation of the effective dipole moment is kind of under simplified condition. That is, the applied electric field outside the particle is taken to be a uniform magnitude E_0 with frequency ω and parallel to z axes (*i.e.* $E(t) = Re[E_0\mathbf{z}e^{j\omega t}]$). The electrostatic potential satisfies Laplace equation everywhere, and the solutions for outside $\phi_1(\mathbf{r},\theta)$ and inside $\phi_2(\mathbf{r},\theta)$ are:

$$\phi_1(r,\theta) = -Er\cos\theta + \frac{A\cos\theta}{r^2}, \quad r > R \tag{2.7}$$

$$\phi_2(r,\theta) = -Br\cos\theta, \quad r < R. \tag{2.8}$$

A and B are unknown coefficients to be determined by the boundary conditions. The first term in the r.h.s of 2.7 is the imposed electric field, and the second term is due to the dipole moment of the particle. There are two boundary conditions at the surface $r = R$. First is that the electric potential should be continuous, that is:

$$\phi_1(r = R,\theta) = \phi_2(r = R,\theta). \tag{2.9}$$

The other is the conservation law of current flux. That is,

$$J_{r1} - J_{r2} + \frac{\partial\sigma_f}{\partial t} = 0, \quad r = R$$

where $J_{r1} = \sigma_m E_{r1}$ and $J_{r2} = \sigma_p E_{r2}$ are the normal components of the ohmic current outside and inside the sphere, σ_f is the free electric surface charge, which can be expressed as:

$$\sigma_f = \epsilon_m E_{r1} - \epsilon_p E_{r2} \tag{2.10}$$

Solving those boundary conditions, A is obtained:

$$A = \frac{\epsilon_p^* - \epsilon_m^*}{\epsilon_p^* + 2\epsilon_m^*} R^3 E_0, \tag{2.11}$$

where $\epsilon^* = \epsilon - j\frac{\sigma}{\omega}$, and $j = \sqrt{-1}$. From 2.6 we know:

$$\mathbf{p}_{eff} = 4\pi\epsilon_m A. \tag{2.12}$$

We obtain a general expression for the complex effective moment $\mathbf{p}_{eff}$ for a dielectric sphere with loss in an electric field as the form:

$$\mathbf{p}_{eff} = 4\pi\epsilon_m Re[K] R^3 \mathbf{E}. \tag{2.13}$$

K, the Clausius-Mossotti factor, is given by:

$$K = \frac{\epsilon_p^*(\omega) - \epsilon_m^*(\omega)}{\epsilon_p^*(\omega) + 2\epsilon_m^*(\omega)}. \tag{2.14}$$

K can also be expressed by using the Maxwell-Wagner surface polarization relaxation time τ_{MW}:

$$K(\omega) = K_\infty + \frac{K_0 - K_\infty}{j\omega\tau_{MW} + 1}. \tag{2.15}$$

Here $\tau_{MW} = \frac{\epsilon_p + 2\epsilon_m}{\sigma_p + 2\sigma_m}$. Therefore, the low- and high-frequency limits of K are:

$$K_\infty = \frac{\epsilon_p - \epsilon_m}{\epsilon_p + 2\epsilon_m} \tag{2.16}$$

$$K_0 = \frac{\sigma_p - \sigma_m}{\sigma_p + 2\sigma_m}. \tag{2.17}$$

Consider a homogenous dielectric ellipsoid in a parallel electric field, with the external applied field $\mathbf{E}_0$ oriented arbitrarily with respect to the ellipsoid and with the components E_x, E_y and E_z along the semi-axes of the ellipsoid. The effective dipole moments for an ellipsoid are different in three directions. The x component is [Jones 1995]:

$$(\mathbf{P}_{eff})_x = \frac{4\pi abc}{3}\epsilon_m Re[\frac{\epsilon_p^* - \epsilon_m^*}{\epsilon_p^* + (\epsilon_m^* - \epsilon_p^*)L_x}]E_x. \tag{2.18}$$

Here the depolarization factor L_x is defined by

$$L_x = \frac{abc}{2}\int_0^\infty \frac{ds}{(s+a^2)R_s}, \tag{2.19}$$

where $R_s = \sqrt{(s+a^2)(s+b^2)(s+c^2)}$. The y, z components of effective dipole moment have similar expressions.

2.3. DEP force in a uniform AC field based on EDM

The general expression for electric field of an AC field, can be written as

$$\mathbf{E} = Re[\tilde{\mathbf{E}}(\mathbf{x})e^{i\omega t}], \tag{2.20}$$

where the vector $\tilde{\mathbf{E}}$ is the corresponding complex phasor. Without losing generality, supposing the AC electric field has a constant phase across the system, $\tilde{\mathbf{E}}$ is real. The dipole moment of the spherical particle becomes:

$$\tilde{\mathbf{p}} = 4\pi\epsilon_m\beta R^3\tilde{\mathbf{E}}e^{i\omega t} \tag{2.21}$$

The time-average force acting on the particle is:

$$< \mathbf{F}_{DEP} >= \mathbf{p}_{eff} \cdot \nabla\mathbf{E} = 2\pi R^3\epsilon_m\beta\tilde{\mathbf{E}} \cdot \nabla\tilde{\mathbf{E}}. \tag{2.22}$$

Using a vector identity, $\nabla(\mathbf{A}\cdot\mathbf{B}) = (\mathbf{A}\cdot\nabla)\mathbf{B} + (\mathbf{B}\cdot\nabla)\mathbf{A} + \mathbf{B}\times(\nabla\times\mathbf{A}) + \mathbf{A}\times(\nabla\times\mathbf{B})$, and $\nabla\times\mathbf{E} = 0$ ($\mathbf{E}$ is an irroational field), (2.22) becomes:

$$< \mathbf{F}_{DEP} >= \pi R^3\epsilon_m\beta\nabla(\tilde{\mathbf{E}}\cdot\tilde{\mathbf{E}}) = \pi R^3\epsilon_m\beta\nabla|\tilde{\mathbf{E}}|^2. \tag{2.23}$$

Consider a homogenous ellipsoid having isotropic dielectric permittivity ϵ_p and semi-axes a, b, and c to be aligned with the x, y and z axes.

$$\mathbf{F}_{DEP} = \mathbf{p}_{eff} \cdot \nabla\mathbf{E} = 4\pi abc\epsilon_m Re[K_i]\mathbf{E}_i \cdot \nabla\mathbf{E}, \quad i = x, y, z, \tag{2.24}$$

with the definition $K_i = Re[\frac{\epsilon_p^* - \epsilon_m^*}{3(\epsilon_p^* + (\epsilon_m^* - \epsilon_p^*)L_i)}] \quad i = x, y, z.$

2.4. Torque and orientation in a uniform field based on EFM

The expression for the torque on a homogeneous sphere in term of the effective moment is:

$$\mathbf{T}^e = p_{eff} \times \mathbf{E}. \tag{2.25}$$

The expression of the torque on a homogeneous ellipsoid in a uniform imposed electric field $\mathbf{E}_0$ is a three component vector. The expression for the x component of torque is:

$$T_x^e = \frac{4\pi abc(\epsilon_p^* - \epsilon_m^*)^2(L_z - L_y)E_yE_z}{3\epsilon_m[1 + (\frac{\epsilon_p^* - \epsilon_m^*}{\epsilon_m})L_y][1 + (\frac{\epsilon_p^* - \epsilon_m^*}{\epsilon_m^*})L_z]}, \tag{2.26}$$

where L_x is defined as (2.19).

T_y^e and T_z^e have similar expressions. These expressions of torque reveal that the particle would always tend to align with its longest axis parallel to $\mathbf{E}_0$ [Jones 1995].

However, for lossy particles, it is no longer true that only the longest axis is stable. All three directions become possible depending on the relative conductivity and permittivity. In the high and low limit of the frequency, the stable direction is the longest axis, but in the intermediate frequency range, the other two axes may become stable. This phenomenon has been observed in many experiments on dielectrophoresis of biocells. One example turkey erythrocytes,

which have an ellipsoidal shape with three distinct axes [Zimmermann *et al.* 1985].

2.5. Model of dielectrophoresis of *E.Coli* cell

Usually, biocells are modeled as concentrically layered dielectric ellipsoids. Asami *et al.* (1980) presented a cell model of *E.coli* as an ellipsoid covered with two confocal shells corresponding to the membrane and cell wall as shown in Figure 2.1

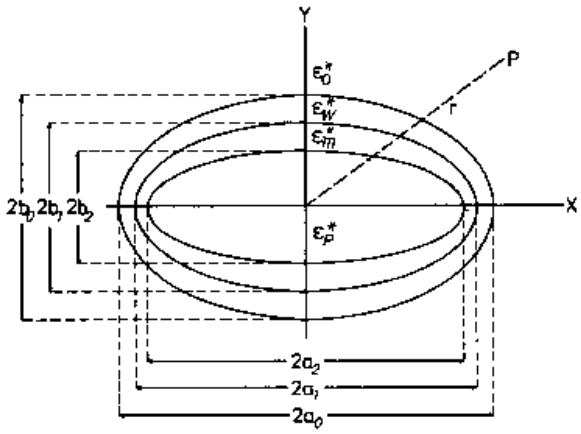

FIGURE 2.1. Cross section of an electrical cell model represented by three confocal ellipsoids in the x-y

The nature of this model is to model a corresponding Clausius-Mossotti factor such that the expression for the dielectrophoretic force can be employed. The details of the derivation is ignored here, and the result is:

$$K_n = \frac{1}{3}\frac{\epsilon^*_{1,n} - \epsilon^*_m}{\epsilon^*_m + (\epsilon^*_{1,n} - \epsilon^*_m)A_n}, \quad n = x, y, z \tag{2.27}$$

$$\epsilon^*_{1,n} = \epsilon^*_w \frac{\epsilon^*_w + (\epsilon^*_{2,n} - \epsilon^*_w)A_n + \lambda_1(\epsilon^*_{2,n} - \epsilon^*_w)(1 - A_n)}{\epsilon^*_w + (\epsilon^*_{2,n} - \epsilon^*_w)A_n - \lambda_1(\epsilon^*_{2,n} - \epsilon^*_w)A_n}, \tag{2.28}$$

$$\epsilon^*_{2,n} = \epsilon^*_m \frac{\epsilon_m * + (\epsilon^*_{p,n} - \epsilon^*_m)A_n + \lambda_2(\epsilon^*_{1,k} - \epsilon^*_w)(1 - A_n)}{\epsilon^*_m + (\epsilon^*_{p,k} - \epsilon^*_m)A_n - \lambda_2(\epsilon^*_{p,k} - \epsilon^*_m)A_n}, \tag{2.29}$$

where

$$\lambda_1 = \frac{(a_0 - d_w)(b_0 - d_w)^2}{a_0 b_0^2}, \tag{2.30}$$

$$\lambda_2 = \frac{(a_0 - d_w - d_m)(b_0 - d_w - d_m)^2}{(a_0 - d_w)(b_0 - d_w)^2}, \tag{2.31}$$

and

$$A_x = -\frac{1}{q^2-1} + \frac{q}{(q^2-1)^{3/2} ln(q+(q^2-1)^{1/2})}, \tag{2.32}$$

$$A_y = A_z = \frac{1}{2}(1-A_x), \tag{2.33}$$

$$q = \frac{a_0}{b_0}. \tag{2.34}$$

Here d_w and d_m are supposed to be the thickness of the cell wall and membrane respectively, other parameters used are indicated in Figure 2.1. Substituting (2.27) into (2.24), the dielectrophoretic force can be calculated.

CHAPTER 3

Modeling and simulation

To simulate the dielectrophoretic phenomena, in this chapter, two models are given. One is fluid dynamics particle method, and the other is a a molecular dynamic approach. They have different applicability.

A very interesting phenomenon of non-spherical cells subjected to dielectrophoretic force is, the orientation of alignment. Then the rotational hydrodynamic force need to be solved properly. Fluid particle dynamics method is a tidy way to deal with particles in flow, which is base of the first model. In addition, we suggest the concept of *effective charge* to incorporate the hydrodynamics with dielectrophoresis into Navier-Stokes equations and solve them.

When the size of particles are much smaller than the length scale of the electrodes, the rotational hydrodynamic force can be ignored and we do not need to solve Navier-Stokes equation. Instead, we suppose that the drag force is given by Stokes law and take the expression for Stokes law directly. This is the case in the applications of separating and collecting particles using dielectrophoretic force. This model therefore is suitable to simulating those processes and used to predict and optimize patterns of design.

3.1. Effective charge and FPD method

3.1.1. *Derivation*

Assuming the frequency of the AC field is within the range where effective dipole moment along long axis dominates, the expression for the dipole moment along this axis is:

$$\mathbf{P}_a = Q\mathbf{d} = 2aQ\mathbf{e}_a, \tag{3.1}$$

where $\mathbf{e}_a$ is the unit vector along the long axis. From (2.18), if we write $\mathbf{E}_a = E_a\mathbf{e}_a$ then we have:

$$\mathbf{P}_a = 4\pi abc\epsilon_m K_a E_a \mathbf{e}_a. \tag{3.2}$$

Here $K_a = Re[\frac{\epsilon_p^* - \epsilon_m^*}{3(\epsilon_p^* + (\epsilon_m^* - \epsilon_p^*)L_a)}]$ From (3.1) and (3.2), we derive the expression for the effective charge:

$$Q = 2\pi bc\epsilon_m K_a E_a. \tag{3.3}$$

Here Q is supposed to be the induced charge in the two ends of the long axis of prolate ellipsoid, with one positive and one negative.

In a fluid particle dynamics model [Tanaka & Araki 2000], a suspension is treated as a completely immiscible fluid mixture, in which very viscous fluid particles with the viscosity η_c are suspended in a liquid component with the viscosity η_s. In the limit of $\frac{\eta_c}{\eta_s} \to \infty$, fluid particles can be regarded as solid ones. Thus, the viscosity ratio $(\frac{\eta_c}{\eta_s})$ is a measure of the accuracy.

The spatial distribution for the viscosity is given by $\eta_c = \eta_s + \Delta\eta$. The viscosity field can be expressed as $\eta(\mathbf{r}) = \eta_s + \sum_i(\eta_c - \eta_s)\phi_i(\mathbf{r})$. The force acting on particle i, is determined as

$$\mathbf{F} = \sum_i \frac{\mathbf{F}_i\phi_i}{\int dr\phi_i}. \tag{3.4}$$

$\phi_i(x)$ is a concentration function which is 1 inside the particle i, and zero outside.

The governing equation we solved, is an equation instead of Navier- Stokes equation with a form as:

$$\begin{aligned} \rho\frac{D\mathbf{u}}{Dt} &= -\nabla p + \nabla\cdot\eta(\nabla\mathbf{u} + \nabla\mathbf{u})^T + \sum_i \frac{\mathbf{F}_i\phi_i}{\int dr\phi_i} \\ &+ \frac{\sum_i \rho_p(d\omega_i \times |\mathbf{r} - \mathbf{r}_i|)\phi_i}{dt}, \end{aligned} \tag{3.5}$$

where ρ_p is the density of particle, ρ is the density of fluid, $\mathbf{F}$ is a total force of all external forces, including the dielectrophoreitc translational force, and $\frac{d\omega}{dt}$ is the rotational motion caused by dielectrophoretic torque. By this way, we coupled the dielectrophoretic force with the hydrodynamic forces properly.

We know, the electrostatic force can be expressed as:

$$\mathbf{F} = \pm Q\mathbf{E}. \tag{3.6}$$

Here $\mathbf{F}$ has the same direction as the local electric field in positive charge point, and has the reverse direction as local electric field in the negative charge point.

If we note $\mathbf{F}_n$ as the point force in the negative charge point and $\mathbf{F}_p$ as positive charge point respectively, we decompose $\mathbf{F}_{p/n}$ into:

$$\mathbf{F}_{p/n} = \mathbf{F}_{p/n,\parallel} + \mathbf{F}_{p/n,\perp}. \tag{3.7}$$

Here $\mathbf{F}_\parallel$ is the component which is parallel to the long axis, and $\mathbf{F}_\perp$ is the component which is perpendicular to the long axis.

Assuming the angle between long axis and the electric field in the negative charged point to be θ and the angle between the long axis and the electric field in positive charged point to be α (in a uniform electric field, $\alpha = \theta$), we obtain the magnitude of the forces as:

$$F_{n,\perp} = F_n\sin\theta, \quad F_{n,\parallel} = F_n\cos\theta, \tag{3.8}$$

$$F_{p,\perp} = F_p\sin\alpha, \quad F_{p,\parallel} = F_p\cos\alpha. \tag{3.9}$$

In 2D case, Γ has only one component:

$$\Gamma = I\frac{d\omega}{dt}. \tag{3.10}$$

I is the rotational inertial. Hence, the angular acceleration caused by the applied electric field can be written as:

$$\frac{d\omega}{dt} = \frac{\Gamma}{I} = \frac{a\mathbf{e}_x \times (F_{p,\perp} + F_{n,\perp})}{I}. \tag{3.11}$$

We also obtain the translational acceleration caused by the applied electric field:

$$\frac{md\mathbf{u}_{\parallel}}{dt} = \mathbf{F}_n \cos\theta + \mathbf{F}_p \cos\alpha, \tag{3.12}$$

$$\frac{md\mathbf{u}_{\perp}}{dt} = \mathbf{F}_n \sin\theta + \mathbf{F}_p \sin\alpha. \tag{3.13}$$

If (3.11), (3.12), and (3.13) are substituted into (3.5), then both the rotational and translational motions of particles can be coupled with hydrodynamic forces properly. We obtain,

$$\begin{aligned}\rho\frac{D\mathbf{u}}{Dt} &= -\nabla p + \nabla\cdot\eta(\nabla\mathbf{u} + \nabla\mathbf{u})^T + \sum_i \frac{\mathbf{F}_i\phi_i}{\int dr\phi_i} \\ &+ \sum_i \rho_p(\frac{\Gamma_i}{I_i} \times |\mathbf{r} - \mathbf{r}_i|)\phi_i,\end{aligned} \tag{3.14}$$

it can be easily solved by FemLego [Amberg *et al.* 1999].

The charge definition is derived from the effective dipole moment expression. Based on it, the values of the local electric field at the ends of long axis are included in the calculation. The size and shape of particles are taken into account by this way. In a uniform electric field, the expressions are equivalent to those based on effective dipole moment. That is, dielectrophoretic force is zero, and the expressions for torque are the same. Figure 3.1 shows the orientational alignment of two elliptic particles in a nonuniform electric field. Figure 3.1(a), 3.1(c), 3.1(e) show the isolines of electric potential, and the changes of the orientation angles of particles in different time moments. As the result of rotation, the angle between long axes and the electric field are parallel (that is, perpendicular to the electric potential), which is what we expected. Figure 3.1(b), 3.1(d), 3.1(f) show the velocity fields at different time moments. From Figure refcha3.1.b, we see the velocity inside the upper particle are much smaller than that in the lower particle. This is because the angles between the long axes and the electric field which determines the rotational effects are different. ((3.8), (3.9) have revealed the relationship between the magnitude of rotational forces and the orientation angle) Figure 6.6(d) shows that after some time, the lower particle has rotated a lot, and the upper particle gets large rotational motion. Figure 3.1(f) shows that while the two particles arrive

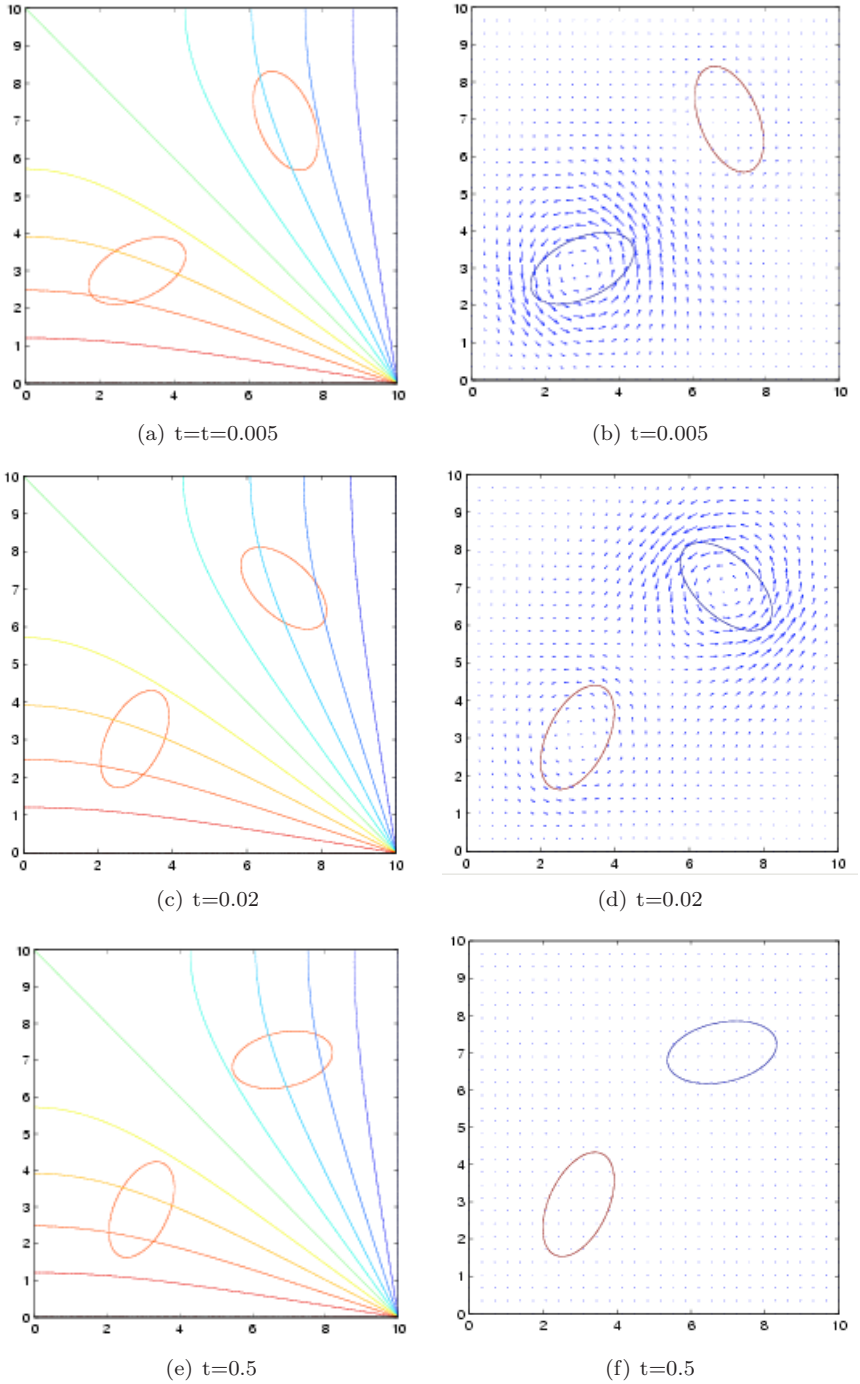

(a) t=t=0.005 (b) t=0.005

(c) t=0.02 (d) t=0.02

(e) t=0.5 (f) t=0.5

FIGURE 3.1. Velocity fields in a nonuniform electric field

the equilibrium positions, the velocities of the particle and the flow are almost zero.

3.2. Molecular dynamics method

In this model, instead of using multi-phase models, we use a molecular dynamics (MD) method [Elimelech *et al.* 1995]. It provides a way of solving the equations of the motion of each particle by replacing them by a set of finite difference equations which are solved on a step-by-step basis.

We view the particles as spheres and consider particles with size much smaller than the length scale of the electrodes. Under such conditions, we do not consider the rotational motion of particles. On the micro level, we consider the flow to be Stokes flow. There will be no need to solve the Navier-Stokes equations. The reason is that according to the specified micro-scale condition, the analytical expression for the hydrodynamic forces between suspended particles in Stokes flows has been well established. Those functions could be directly adopted to account for the hydrodynamic interaction between particles. Besides, since we assume the particles to be spherical and without deformation, it is reasonable to just add repelling forces which become significant when two particles come close. The net DEP forces acting on the particles by the field and the interactive electrostatic forces from other particles can also be added on the centers of mass of the particle. Therefore, we are able to include all the forces into a set of coupled equation of motion (ordinary differential equations) for many-body systems. We do not need to solve the Navier-Stokes equation if we are not interested in the fluid itself.

3.2.1. *Analysis of inertial effect*

For simplification, we suppose a sphere in a fluid flow with speed v is subjected to an external force $\mathbf{F}$. According to Newton Second Law:

$$m\frac{d\mathbf{u}}{dt} = \mathbf{F} - 6\pi\mu a(\mathbf{u} - \mathbf{v}) \tag{3.15}$$

The second term of (3.15) is the Stokes drag force that the sphere is subjected to from the fluid [Morgan & Green 2001], $\mathbf{u}$ is the speed of particle, m is the mass of the sphere, and μ is the viscosity of fluid. The solution for the speed of the particle, $\mathbf{u}$, can be easily obtained:

$$\mathbf{u} = (\mathbf{u}_0 + \mathbf{v} + \frac{\mathbf{F}}{6\pi\mu r})e^{-(\frac{6\pi\mu a}{m})t} \tag{3.16}$$

It is reasonable to take the characteristic time as $\tau = \frac{m}{6\pi\mu a} = \frac{2\rho a^2}{9\mu}$. If the density of cells, ρ, is taken as the same as water, and the fluid viscosity is taken as water, then $\tau \approx 10^{-6}$ s. Since the limit of time for observation is about 1/30 s, which is much longer than τ, therefore, the particle that is observed moves at the terminal speed. For nanoparticles, the characteristic time τ is even smaller.

This means that, in microsystems, the inertial effect is negligible, which is a basic assumption for our molecular dynamic approach.

3.2.2. *Hydrodynamic interaction*

One of the aims in this paper was to take the hydrodynamic force into account. The governing equations of the motion of an incompressible fluid, the Navier-Stokes equations, could be non-dimensionalized as Kundu & Cohen (2002):

$$Re(\frac{\partial \mathbf{U}}{\partial t} + \mathbf{U} \cdot \nabla \mathbf{U}) = -\nabla p + \nabla^2 \mathbf{U} + \mathbf{f} \tag{3.17}$$

$$\nabla \cdot \mathbf{U} = 0 \tag{3.18}$$

where Re is the Reynolds number defined as $Re = \frac{UL}{\nu}$, which determines the relative importance of the fluid inertia and viscous forces. However, in micro flows when $R << 1$ and under steady state, the nonlinear terms can be neglected, and by further assuming that external forces are absent, the governing equations can be written as:

$$\nabla^2 \mathbf{U} = \nabla p, \tag{3.19}$$

$$\nabla \cdot \mathbf{U} = 0, \tag{3.20}$$

which are known as the Stokes or creeping flow equations. The motion of a given particle induces a flow field in the solvent, which will be felt by every other particle. As a result, these particles experience a force which can be said to result from the hydrodynamic interaction with the original particle. By solving the Stokes equation for a two-particle case, the first expression for the mobility tensor, as given by Oseen [Elimelech *et al.* 1995], is:

$$\mu_{ij} = \delta_{ij} \frac{1}{6\pi\mu a} + (1 - \delta_{ij}) \frac{1}{8\pi\mu r} (\mathbf{1} + \frac{\mathbf{r}_{ij}\mathbf{r}_{ij}}{r_{ij}^2}), \tag{3.21}$$

where $\mathbf{1}$ is the unit tensor, $\mathbf{r}_{ij} = \mathbf{r}_i - \mathbf{r}_j$, $r_{ij} = |\mathbf{r}_i - \mathbf{r}_j|$, and δ_{ij} is the Kronecker delta. Therefore, we get the velocity expression as:

$$\mathbf{U}_i = -\sum_{j=1}^{N} \mu_{ij} \cdot \mathbf{F}_j \tag{3.22}$$

Corrections resulting from n-body interactions ($n \geq 3$) need not to be taken into account. That is, for example, particle A can affect particle C directly and affect C indirectly by affect particle B and B can therefore effect particle A. The indirect influences are expressed by correction functions of the order $(\frac{a}{r_{ij}})^2$ or higher [Elimelech *et al.* 1995]. The hydrodynamic force acting on particle i can be expressed as:

$$\mathbf{F}_{drag,i} = -\sum_{j=1}^{N} \zeta_{ij} \cdot \mathbf{U}_j \tag{3.23}$$

where tensor η_{ij} is defined as:

$$\zeta_{ij} = \delta_{ij}(6\pi\mu a) + (1-\delta_{ij})6\pi\mu a\frac{3a}{4r_{ij}}(\mathbf{1} + \frac{\mathbf{r}_{ij}\mathbf{r}_{ij}}{r_{ij}^2}) \tag{3.24}$$

To maintain stability and to avoid the time step restrictions of explicit methods, the velocity $\mathbf{U}i$ in (3.22) is discretized by using an implicit scheme. Therefore, a nonlinear system of equations must be solved.

3.2.3. *Electrostatic interaction*

For an isolated spherical particle subjected to an electric field $\mathbf{E}$, the polarization is given by

$$\mathbf{p} = 4\pi\epsilon_m\beta a^3\mathbf{E} \tag{3.25}$$

β is the real part of Causius-Mossotti factor, a is the radius of particle, To obtain the interaction forces between particle i and j, we have the expressions for the dipole moment of these particles as:

$$\mathbf{p}_i = 4\pi\epsilon_m\beta a^3\mathbf{E}_i, \quad \mathbf{p}_j = 4\pi\epsilon_m\beta a^3\mathbf{E}_j, \tag{3.26}$$

where $\mathbf{E}_i$ and $\mathbf{E}_j$ are electric field intensity at the positions of centers of particle i and j. Witten in vector form , the expression of electrostatic interactions $\mathbf{F}_{D,ij}$ is:

$$\begin{aligned}\mathbf{F}_{D,ij} &= \frac{1}{4\pi\epsilon_m}\frac{3}{r^5}(\mathbf{r}_{ij}(\mathbf{p}_i\cdot\mathbf{p}_j) + (\mathbf{r}_{ij}\cdot\mathbf{p}_i)\mathbf{p}_j \\ &\quad +(\mathbf{r}_{ij}\cdot\mathbf{p}_j)\mathbf{p}_i - \frac{5}{r^2}\mathbf{r}_{ij}(\mathbf{p}_i\cdot\mathbf{r}_{ij})(\mathbf{p}_j\cdot\mathbf{r}_{ij}))\end{aligned} \tag{3.27}$$

After non-dimensionalization, it can be expressed as:

$$\begin{aligned}\frac{d\mathbf{x}_i}{dt} &= P_1\mathbf{FG}_{i,j}\cdot\frac{d\mathbf{x}_j}{dt} + P_2\mathbf{FD_i} + P_3\mathbf{FDIP_{ij}} \\ &\quad +\mathbf{F}_{W,i} + \mathbf{F}_{P,i}\end{aligned} \tag{3.28}$$

with the following definitions:

- Characteristic variables:

  L: Length V_0: Potential T: Time
- Dimensionless parameters:

$$P_1 = \frac{3r}{4L}, \quad P_2 = \frac{2\beta r^2\epsilon_m V_0^2 T}{3L^4\mu} \quad P_3 = \frac{2\epsilon_m\beta^2 r^5 V_0^2 T}{\mu L^7} = 3\beta(\frac{r}{L})^3 P_2$$

- Dimensionless functions

$$\begin{aligned} \mathbf{FD}_i &= \nabla|\mathbf{E}^*|^2 \\ \mathbf{FG}_{ij} &= \frac{1}{R^*_{ij}}(\mathbf{1} + \hat{\mathbf{R}}^*_{ij}\hat{\mathbf{R}}^*_{ij}) \\ \mathbf{FDIP}_{ij} &= \frac{1}{(R^*_{ij})^5}(\mathbf{R}^*_{ij}(\mathbf{p}^*_i \cdot \mathbf{p}^*_j) + \\ (\mathbf{R}^*_{ij} \cdot \mathbf{p}^*_i)\mathbf{p}^*_j + (\mathbf{R}^*_{ij} \cdot \mathbf{p}^*_j)\mathbf{p}^*_i &- \frac{5}{(R^*_{ij})^2}\mathbf{R}^*_{ij}(\mathbf{p}^*_i \cdot \mathbf{R}^*_{ij})(\mathbf{p}^*_j \cdot \mathbf{R}^*_{ij})) \end{aligned} \quad (3.29)$$

where **FG** is the dimensionless hydrodynamic force, **FD** is the dimensionless DEP force, **FDIP** is the dimensionless electrostatic force, and $\mathbf{F}_{p,i}$ is the repulsive forces between particles. From the definition of P_1,P_2 and P_3, and (3.28), the scaling relationship between DEP forces and hydrodynamic force can be determined.

Figure 3.3 shows experimental results of *E. coli* bacteria under dielectrophoresis. The electrodes are seen as the v-shaped structures at top and bottom. The bacteria accumulate near the electrode tips, as expected, since these are the points with the largest field gradients. Furthermore they organize into long chains, extending along the electric field lines. This is due to the fact that, under the present conditions, with an AC frequency giving positive DEP, the particles polarize in such a way that they will be negatively charged at the end near the positive electrode, and vice versa. This will create attractive interparticle forces between these induced dipoles. Finally the particles form the long chains along the field lines. Figure 3.2 shows the simulation results. They are in good agreement with the experimental results.

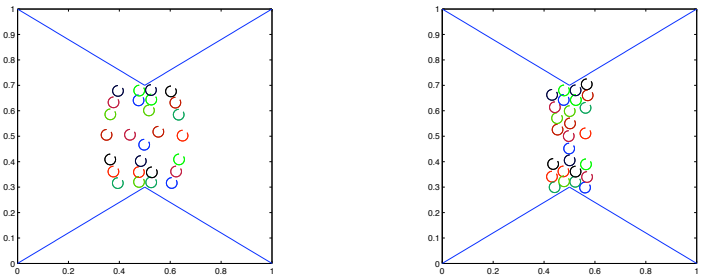

FIGURE 3.2. Particle distribution under pDEP conditions

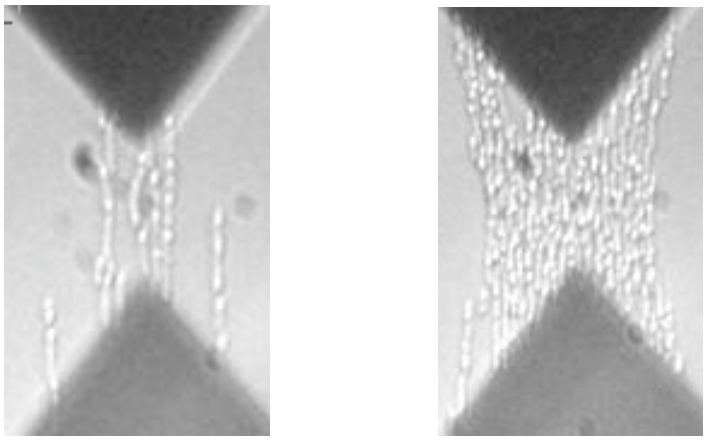

FIGURE 3.3. Alignement of E. coli bacteria under pDEP conditions

3.3. Applications

In the following, we have used our simulations based on molecular dynamics approach to investigate different possible separation techniques. Particle-particle interactions are neglected in the model since we have shown that when the gradient of electric field is high, the interactive forces are negligible compared to dielectrophoretic forces.

3.3.1. *Superposition dielectrophoretic forces*

We apply our model in the calculation for enhancing the trapping efficiency of *E.coli* cells. In this problem, the Clausius-Mossotti factor is a frequency-dependent complex number with the real part value between -0.5 and 1. We showed that if proper superimposed electric fields (with different frequency) are used in the calculation, the trapping efficiency can be enhanced greatly.

Below is the simple mathematical proof of the validity of superposition of dielectrophoretic forces:

For one single frequency the DEP force is quadratic in the electric field, as (2.23). Since $\mathbf{E} = \nabla\tilde{\phi}$ ($\tilde{\phi}$ is the potential of electric field which can be written as $\tilde{\phi} = \phi \sin \omega t$ with ϕ only depends on space), after nondimensionlization, we get the relationship between $\mathbf{F}_{dep}$ and potential ϕ as:

$$\mathbf{F}_{dep} = \nabla(\nabla\phi \sin(\omega t))^2. \tag{3.30}$$

The time average force is then:

$$< \mathbf{F} > = \frac{1}{T}\nabla(\nabla\phi)^2 \int_0^T \sin^2(\omega t) \tag{3.31}$$

$$= \frac{1}{2}\nabla(\nabla\phi)^2. \tag{3.32}$$

Suppose two harmonic potentials with different frequencies are introduced at the same time to a system, we have the superimposed electric potential as:

$$\tilde{\phi}_{total} = \phi_1 \sin(\omega_1 t) + \phi_2 \sin(\omega_2 t) \tag{3.33}$$

therefore,

$$(\nabla\tilde{\phi}_{total})^2 = (\nabla\phi_1 \sin(\omega_1 t) + \nabla\phi_2(\omega_2 t))^2 \tag{3.34}$$

$$= \nabla\phi_1^2 \sin^2(\omega_1 t) + \nabla\phi_2^2 \sin^2(\omega_2 t) + 2\nabla(\phi_1 \sin(\omega_1 t)\nabla\phi_2 \sin(\omega_2 t)$$

The time-average force is:

$$< \mathbf{F} >_{total} = \frac{1}{T}\int_0^T F_{dep} dt$$

$$= \frac{1}{T}\nabla(\nabla\phi_1)^2 \int_0^T \sin^2(\omega_1 t)dt + \frac{1}{T}\nabla(\nabla\phi_2)^2 \int_0^T \sin^2(\omega_2 t)dt$$

$$+ 2\frac{1}{T}\nabla(\nabla\phi_1\nabla\phi_2) \int_0^T \sin(\omega_1 t)\sin(\omega_2 t)dt \tag{3.35}$$

When T tends to infinity, it is easy to verify that the last term of 3.35 tends to zero, and 3.35 becomes:

$$< \mathbf{F} >_{total} = \frac{1}{2}\nabla(\nabla\phi_1)^2 + \frac{1}{2}\nabla(\nabla\phi_2)^2 = < \mathbf{F} >_1 + < \mathbf{F} >_2 \tag{3.36}$$

Therefore, it is correct to superimpose the DEP forces corresponding to superimposed AC fields of different frequencies.

As an example, Figure 3.4 shows the traces of *E.coli* cells under DEP forces in a rectangular channel. Three different electrode configurations were considered. A Poiseuille flow enters the channel from the left. Particles are released from different positions through the channel cross section. In configuration A, only the electrodes at the bottom of the channel are used. The frequency of the AC field is chosen to give a positive DEP, i.e. particles are attracted to regions of high field gradients. In configuration B, both the electrodes at the bottom and the top were turned on at a voltage frequency where the particles only obtain a positive dielectrophoretic motion. In configuration C, both the electrodes are turned on, but different frequencies are utilized. The bottom electrodes have a frequency inducing positive DEP, and the top electrodes have a frequency inducing negative motion. The trapping rate of configuration B is 100%, which proves configuration B is the best one in this condition.

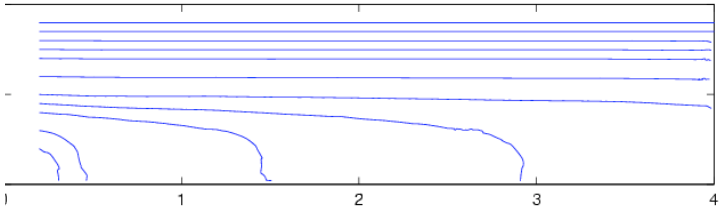

(a) performed in the pDEP mode at the bottom.

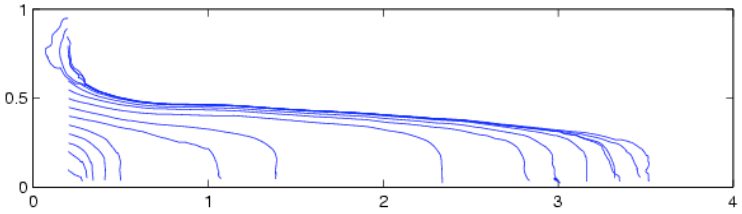

(b) with pDEP both at the bottom and at the top.

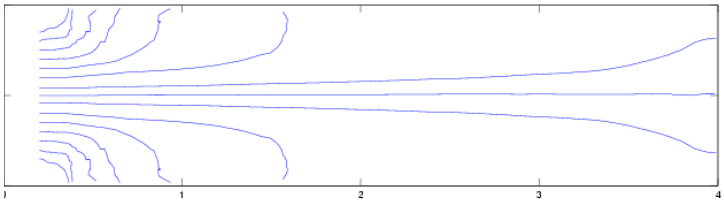

(c) with pDEP at the bottom and nDEP at the top.

FIGURE 3.4. Particle trajectories in a high conductivity solution.

3.3.2. *Multi-step dielectrophoresis*

The idea of multi-step dielectrophoresis is, by repeating the trapping-release process, particles with small difference in size and dielectrophoretic properties can be separated. Figure 3.5 is a schematic of this strategy. To quantify the degree of fractionation separated, a concept as the *dielectrophoretic resolution* (R_{DEP}) is defined as:

$$R_{DEP} = \frac{3d}{w_A + w_B} \tag{3.37}$$

where d is the distance between the two centers of each particle population, and w is the band width of the particle population. It is easy to understand, when $R_{DEP} > 1.5$, the two particle populations will be completely separated, because it is equivalent to:

$$d > \frac{w_a + w_b}{2} \tag{3.38}$$

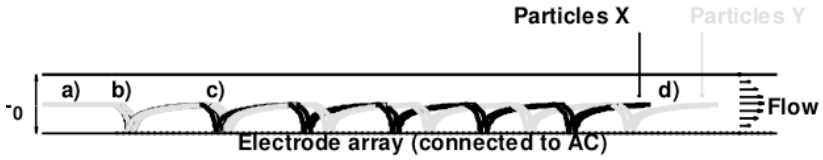

FIGURE 3.5. A schematic of a polarisable particle suspended within a point-plane electrode system. When the particle polarises, the interaction between the dipolar charges with the local electric field produces a force.

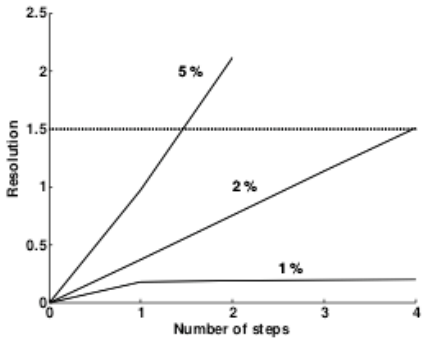

FIGURE 3.6. Calculated resolution as a function of number of steps for a relative difference in size of 5%, 2% and 1%.

For example, Figure 3.6 shows that a complete separation can be achieved in two steps if the difference in size is 5%. If the size difference is 0.5%, 20 steps are required (Figure 3.7). If the size difference is 0.2%, 200 steps are need (Figure 3.8).

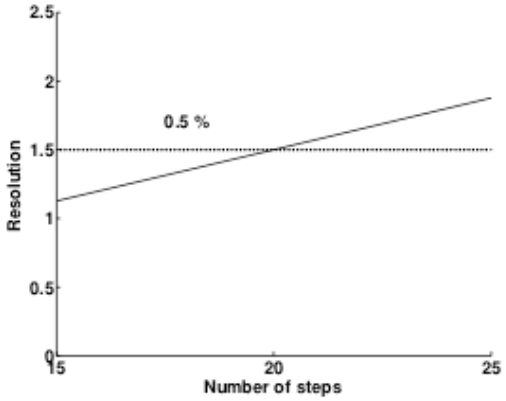

FIGURE 3.7. Calculated resolution as a function of number of steps for a relative difference in size of 0.5 %.

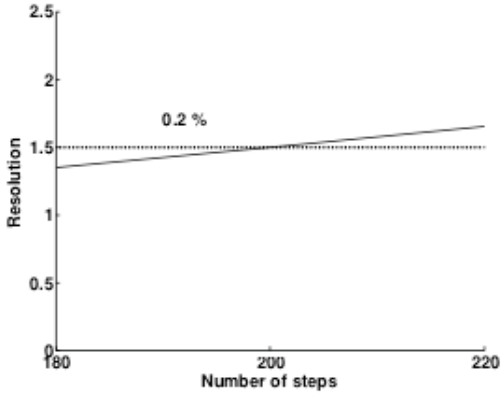

FIGURE 3.8. Calculated resolution as a function of number of steps for a relative difference in size of 0.2 %.

CHAPTER 4

Summary of papers

Paper 1

In this paper, the author suggested the concept as *effective charge* and based on which derived the expression for dielectrophoretic force and torque. Fluid particle dynamics method is modified to simulate the motion of non-spheric particles in fluid. By coupling the dielectrophoresis expressions with the fluid particle dynamics method, the author simulated the motion of two ellipsoidal particles in a uniform and nonuniform electric field respectively. This method was originated while somewhat different from the widely used ways which are based on the effective dipole moment. An investigation between the time scales of different dielectrophoretic motions are also carried out.

Paper 2

A molecular dynamics approach is suggested in this paper based on the point-approximation effective dipole moment. A set of equations of motion of micro-size particles based on the Newton second law are solved step by step with inertial effects neglected. Translational hydrodynamic force corrections of Stokes flow are coupled with dielectrophoretic force together with the particle-particle electrostatic interaction and the particle-particle interface repulsion.

Paper 3

A simpler version of the molecular dynamic approach in paper 2 is used to calculate the dielectrophoresis force which *E.coli* cells are subjected to in 3D. Superimposed AC electric fields of different frequencies are used to give nDEP and pDEP forces simultaneously. The interactions between particles are ignored because when the gradient of electric field is high and when the length scale of electrodes is much larger than the size of particles, the interactions are trivial. The results shows that applying the superimposed electric fields properly enhances the trapping efficiency greatly.

Paper 4

The model used in this paper is the same as that in paper 3. A multi-step trapping-releasing mechanism is utilized to separate the particles with differences in size and dielectrophoretic properties. Results shows that the mechanism can separate particles with much smaller difference in size and dielectrophoretic properties than traditional ways.

CHAPTER 5

Conclusions and outlook

This thesis contains two methods to model and simulate the dielectrophoretic phenomena of microparticles, as well as two applications in the design of the microchannel for cell separating.

In the first model, the fluid particle dynamics method coupled with dielectrophoretic forces and torque is used. The rotational motions of ellipsoidal particles in a uniform and nonuniform electric field are observed as well as the motion of the fluid around. The particle-particle interactions are also calculated. However, it is rather expensive to apply in the calculation of DEP applications. The reason is, the time scale of rotational motion is much smaller than that of translational motion.

The second model is based on the widely used point-approximation effective dipole moment method. A molecular dynamic approach is suggested to simulate the particle motions. The rotational motions of particles are neglected since the size of particles is much smaller than the length scale of the electrodes. The particle-particle interaction forces (including hydrodynamic and electrostatic forces) are incorporated as well as the DEP forces. An investigation between DEP forces and interactios is carried out based as well.

The molecular dynamic method with the interactions neglected is used to calculate dielectrophoretic motions of particles in a microchannel with carrier flow. The first application shows that superimposed external electric fields can enhanced the trapping rate of *E. Coli* cells greatly. The second application reveals that by using this multi-step trapping-releasing mechanism, particles with much smaller difference in size and dielectrophoretic properties can be separated than traditional ways.

In the future work, for the fluid particle model, concentration field functions can be carried out to simulate different shape objects. A big challenge is to simulate objects with flexible interface. A non-conservative phase field method probably may be a good model for the concentration field. For the molecular model, Brownian motion and Van Der Waals forces can be incorporated to simulate nanoparticles. Since the surfaces of most of nanoparticles in solution are charged, the electric double layer also plays an important role. Coupling the electric double layer effect into the dielectrophretic model is necessary and also a challenge. Severe difficulty in experimental aspect may be that the

physical and chemical parameters needed in mathematical models are difficult to measure. Maxwell stress tensor method can also be a choice to improve the accuracy of calculation for dielectrophoretic force and torque, especially for particles whose size is comparable to the size of electrodes.

Acknowledgements

My supervisor Prof. Gustav Amberg deserves many thanks and a deep appreciation. He has been an inspiring source and a role of model for me even when I was doing my master thesis. His keen insight to the nature of the phenomena, abundant knowledge and experiences have never stopped impressing me and supporting me. He also taught me patience. Besides, I thank him for guiding me of skiing and sharing the relaxing summer afternoon in his garden.

Furthermore, I would like to thank my collaborators Fredrik Aldaeus and Prof. Johan Roeraade at Department of Chemistry, for nice collaborations.

I also thank all of my colleagues at Department of Mechanics for contributing a comfortable and pleasant working atmosphere. Especially, Dr. Minh Do-Quang, Walter Villanueva, for not only sharing the office room, but also their knowledge and experiences. Jerome Hœpffner, Tobias Strömgren, Ramis Örlü are appreciated for suggestions and discussions, Ingunn Wester for dealing with my personal requirements.

Dr. Junichiro Shiomi from Tokyo University is thanked for the working time together on carbon nanotube. Prof. Shi-li Zhang is acknowledged for stimulating discussion and pleasant conversations. Dr. Zhi-bin Zhang is thanked for sharing many interesting papers and discussions.

I wish to express my gratitude to all my friends in Sweden, especially Yu Tian and Kun Zhu for their amazing cooking which pleases me a lot. I thank my parents who have been encouraging and supporting me all the way. Special thanks are conveyed to my husband Ming Xiao, for his love, support, company and proof reading of part of the thesis.

The Swedish Research Council (VR) is gratefully acknowledged for the financial support.

Bibliography

Amberg, G., Tönhardt, R. & Winkler, C. "Finite element simulations using symbolic computing" *Math. Comp. Simulation* 49, 257-274, 1999.

Asami, K., Hanai & T., Koizumi, N. "Dielectric analysis of escherichia coli suspensions in the light of the theory of interfacial polarization ", *Journal of Biophys* 31, 215-228, 1980

Asbury, C. L. & Engh, G. V. D. "Trapping of DNA in nonuniform oscillating electric fields", *Biophysical Journal* 74, 1024-1030, 1998

Asokan, S. B., Jawerth, L., Lloyd Carroll, R., Cheney, R. E., Washburn, S., & R. Superfine, R. "Two-dimensional manipulation and orientation of actinmyosin systems with dielectrophoresis ", *Nano Lett.* 3, 431, 2003.

Batchelder, J. S., *Rev. Sci. Instrum* 54, 300-202, 1983

Becker, F. F., Wang, X., Huang, Y., Pethig, R., Vykoukal, J. & Gascoyne, P. R. C "Separation of human breast cancer cells from blood by different dielectric affinity", *Proc. Natl. Acad. Sci. USA.* Volume 82, 860-864, 1995

Dimaki, M. & Bøggild P. "Dielectrophoresis of carbon nanotubes using microelectrodes: a numerical study", *Nanotechnology* 15, No8, 1095-1102, 2004

Elimelech, M., Gregory, J., Jia, X. & Williams. R. A. , "Particle Deposition and Aggregation - Measurement, Modelling and Simulation", *Elsevier USA*, 219-220, 1995

Gascoyne, P. R. C., Wang, X. B., Huang, Y. & Becker, F. F. "Dielectrophoretic Separation of Cancer Cells from Blood", *IEEE transactions on industry applications* 33, 670-678, 1997.

Gascoyne, P. R. C., Huang, Y., Pethig, R., Vykoukal, J. & Becker F. F. "Dielectrophoretic separation of mamalian cells studied by computerized image analysis ", *SC. Technol.* 3, 439-445, 1992.

Glowinski, R., Pan, T. W., Hesla, T. I., Joseph, D. D. & Periaux, J. "A Fictious Domain Approach to the Direct Numerical Simulation of Incompressible Application to Particulate Flow", *Journal of Computational Physics* 169, 363-426, 2001.

Green, N. G. & Morgan, H. "Dielectrophoresis of submicrometer latex spheres. I: Experimental results", *J. Phys. Chem.* B 103. 41, 1999.

Huang, J. P., Karttunen, M., Yu, K.W. & Dong, L. "Dielectrophoresis of charged colloidal suspensions ", *Phy. Rev E* 64, 021401, 2002

Hunter, R. J., "Zeta Potential in Colloid Science ", *London Academic*, 1981

Jones, T. B. "Electromechanics of Particles", *Cambridge University Press, UK*, 34-49, 1995.

Kadaksham, J., Singh, P. & N. Aubry "Manipulation of particles using dielectrophoresis", *Mechanics Research Communications* 33, 208-122 2005

Kadaksham,A. T. J., Singh, P. & Nadine Aubry "Dielectrophoresis of nanoparticles", *Electrophoresis* 25, 3625-3632, 2004

Karniadakis, GEM & Beskok, A, "Micro Flows. Fundamentals and Simulation", *Springer-Verlag*, 2002.

Krupke, R., Hennrich,, Löhneysen, H. V. & Kappes, M. M. "Separation of metallic from semiconduction-single-walled carbon nanotubes", *Science* 301, 344, 2003a

Krupke, R. Hennrich, F., Weber, H. B., Kappes, M. M. & Löhneysen H. V. "Simultaneous Deposition of Metallic Bundles of Single-walled Carbon Nanotubes Using AC-dielectrophoresis", *Nano Letter* 3, 1019-1023, 2003b

Krupke, R., Hennrich, F., Kappes, M. M. & Löhneysen, H. V. "Surface Conductance induced Dielectrophoresis of Semiconducting Single-Walled Carbon Nanotubes", *Nano Letters* 4, 1395-1399, 2004

Kundu, P. K. & Cohen, I. "Fluid Mechanics ", *Academic Press* 4, 97-99, 2002

Liu, H. & Bau H. H. "The dielectrophoresis of cylindrical and spherical particles submerged in shells and in semi-infinite media ", *Physics of fluid* 16, No5, 1217-1228, 2004

Lyklema, J. "Fundamentals of Interface and Colloid Science ii", *London Academic*, 1995

Markx, G. H., Dyda, P. A. & Pethig, R. "Dielectrophoretic separation of bacteria using a conductivity gradient ", *Journal of Biotechnology* 51, 175-180, 1996.

Markx, G. H., Pethig, R. & Rousselet, J. "The dielectrophoretic levitation of latex beads, with reference to field-flow fractionation", *Journal of Physics* 30, 2470-2477, 1997.

Morgan, H. & Green N. G. "Dielectrophoretic manipulation of rodshaped viral particles ", *Journal of Electrostatics* 42 279-293, 1997.

Morgan, H., Green, N. G., Hughes, M. P., Monaghan, W. & Tan, T. C. "Large-area travelling-wave dielectrophoresis particle separation", *Journal of micromechanics and Microengineering* 7 65-70, 1997.

Morgan, H., Green, N. G. "AC Electrokinetics: Colloids and Nanoparticles", *Research Studies Press, UK* 50-54, 2001.

Pohl, H. A. "The motion and precipitation of suspensoids in divergent electri fields", *Journal of Applied Physics* 22, 155-181, (1951).

Pohl, H. A. "Dielectrophoresis", *Cambridge University Press, UK* 6-15, 1978.

Romos, A., Morgan, H., Green, N. G. & Castellanos, A. "Ac electrokinetics: a review of forces in microelectrode structures ", *J. Phys. D: Applied Phys.* 4, 31 2338-53, 1999

Sauer, F. A., "Forces on suspended particles in the electromagnetic field ", *Coherent excitations in biological systems* Berlin: Springer-Verlag, 134-144, 1983

Tanaka, H. & Araki, T. "Simulation method of Colloidal Suspensions with Hydradynamic Interactions: Fluid Particle Dynamics", *Physical Review Letters, UK* 85. 1338-1341, 2000.

Wang, X. J., Wang, X. B., & Gascoyne P. R. C. "General expressions for dielectrophoretic force and electrorotational torque derived using the Maxwell stress torque ", *Journal of Electrostatics* 39, 277-295, 1997

Washizu, M., Washizu, M. & Kurosawa, O "Electrostatic manipulation of DNA in microfabricated structures ", *IEEE Trans. Ind. Electron.* 26, 1165, 1990

Washizu, M., Suzuki, S., Kurosawa, O., Nishizaka, T. & Shinohara, T. "Molecular dielectrophoresis of biopolymers ", *IEEE Trans. on Ind. Appl.* 30, 835-843, 1994

Yang, J., Huang, Y., Wang, X. B., Becker, F. F. & Gascoyne, P. R. C. "Cell separation on microfabricated electrodes using dielecgtrophoreticgravitational field-flow-fraction", *Analytical Chemistri* 71, 911-918, 1999

Zimmermann, U., Vienken, J., & Pilwat, G. "Electrofusion of cells", *Inverstigative Microtechniques in Medicine and Biology* 89-167, 1985.